CHIN. PHYS. LETT. Vol. 36, No. 2 (2019) 028102 **Express Letter**

Formation of Two-Dimensional AgTe Monolayer Atomic Crystal on Ag(111) Substrate *

Li Dong(董立)[1,2], Aiwei Wang(王爱伟)[1,2], En Li(李恩)[1,2], Qin Wang(汪琴)[1,2], Geng Li(李更)[1,2**], Qing Huan(郇庆)[1,2], Hong-Jun Gao(高鸿钧)[1,2**]

[1] *Institute of Physics, Chinese Academy of Sciences, Beijing 100190*
[2] *University of Chinese Academy of Sciences, Beijing 100190*

(Received 15 January 2019)

We report on the formation of two-dimensional monolayer AgTe crystal on Ag(111) substrates. The samples are prepared in ultrahigh vacuum by deposition of Te on Ag(111) followed by annealing. Using a scanning tunneling microscope (STM) and low electron energy diffraction (LEED), we investigate the atomic structure of the samples. The STM images and the LEED pattern show that monolayer AgTe crystal is formed on Ag(111). Four kinds of atomic structures of AgTe and Ag(111) are observed: (i) flat honeycomb structure, (ii) bulked honeycomb, (iii) stripe structure, (iv) hexagonal structure. The structural analysis indicates that the formation of the different atomic structures is due to the lattice mismatch and relief of the intrinsic strain in the AgTe layer. Our results provide a simple and convenient method to produce monolayer AgTe atomic crystal on Ag(111) and a template for study of novel physical properties and for future quantum devices.

PACS: 81.05.Zx, 68.37.−d, 81.07.−b, 81.15.Ef DOI: 10.1088/0256-307X/36/2/028102

Since the first exfoliation of graphene in 2004,[1] research on 2D atomic crystals has become a hot and expanding topic.[2–6] A lot of materials including the graphene[7–9] family (e.g., silicene,[10–12] germanene,[13] antimonene,[14,15] stanene[16] and borophene[17]), transition-metal dichalcogenides (TMDs),[18–21] metal carbides[22] and others have been synthesized in the recent 15 years. Among them, the Te-based 2D atomic crystals have received particular interests. For example, monolayer tungsten ditelluride (WTe_2), a topologically nontrivial insulator, is reported to host superconductivity under gate control.[19] Structural phase transition is achieved in monolayer molybdenum ditelluride ($MoTe_2$) by electrostatic doping.[23] Silver telluride, on the other hand, has been less studied. Ag_2Te nanocrystals have been demonstrated to be a promising candidate for thermoelectric material[24] and infrared detection.[25] Also, β-Ag_2Te is theoretically predicted to be topologically nontrivial[26,27] and an electronic topological transition in Ag_2Te is observed under high pressure.[28] Although silver telluride film has been experimentally achieved,[29] monolayer silver telluride has not been reported yet. In this Letter, we report the fabrication of monolayer AgTe film on Ag(111) substrate based on molecular beam epitaxy technique.

We conducted all the experiments in a homemade ultrahigh vacuum (UHV) STM system with the base pressure better than 1×10^{-10} mbar. The single crystal Ag(111) (roughness <30 nm, orientation accuracy <0.1°, MaTeck Company) was prepared in ultrahigh vacuum by repeated cycles of Ar^+ ion sputtering and subsequent annealing at 770 K until a clean and atomically flat surface was confirmed by STM imaging. The annealing temperature was measured by an infrared radiation thermometer (Mikron PhotriX^{TM} pyrometer, LumaSense Technologies Company). Te was evaporated with a homemade Knudsen cell (K-cell) evaporator, and the annealing temperature is ∼720 K. After the sample preparation, we performed the in situ LEED and STM characterization. All the STM images were taken in a constant-current mode with a bias applied to the sample. The scanning temperature was 80 K.

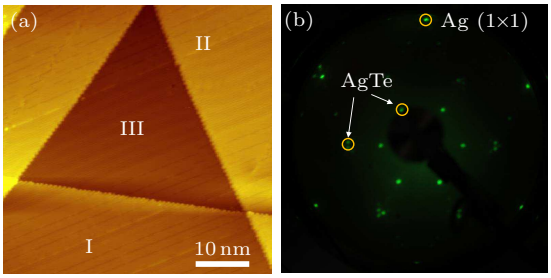

Fig. 1. (a) STM image of large-scale AgTe monolayer on Ag(111) substrate. Scanning parameters: $V_s = -0.6$ V, $I_t = 0.2$ nA. (b) LEED pattern of the sample in (a), with a beam energy of 55.4 eV.

Figure 1(a) shows the large-scale monolayer silver telluride film on Ag(111) substrate. Three different surface regions can be identified. The top and bot-

*Supported by the National Key Research & Development Projects of China under Grant Nos 2016YFA0202300 and 2018FYA0305800, the National Natural Science Foundation of China under Grant Nos 61390501, 61474141 and 11604373, the CAS Pioneer Hundred Talents Program, the Strategic Priority Research Program of Chinese Academy of Sciences under Grant No XDB28000000.

**Corresponding authors. Email: gengli.iop@iphy.ac.cn; hjgao@iphy.ac.cn

tom part show features as alternating rows of ridges and trenches, and the middle part shows the periodical stripe-like features. The trench, ridge and stripe regions and labeled by I, Ⅱ and Ⅲ, respectively. The LEED image is shown in Fig. 1(b). The outer six spots are attributed to the Ag(111) substrate lattice, and the inner spots are assigned to the AgTe overlayer. Multiple sets of diffraction spots also suggest coexistence of different structures of AgTe monolayer.

Figure 2(a) shows the atomic resolution image of the trench regions, and the flat honeycomb structure can be clearly identified. The lattice constants along directions $\boldsymbol{a}$ and $\boldsymbol{b}$ are measured to be 4.85±0.12 Å and 4.68± 0.10 Å, respectively. It should be noted that the piezo of our STM scanner was calibrated by scanning on a standard HOPG substrate. The difference of lattice constants along different high-symmetry directions suggests lattice mismatch between the telluride layer and the substrate as well as the existence of intrinsic in-plane strain in the flat honeycomb area. A line profile is shown in Fig. 2(b), highlighting the cross-sectional information of the topography of the green line in Fig. 2(a). The asymmetry of the two sublattices can be resolved. Based on the above discussions, we speculate that the flat honeycomb area is in fact formed by Ag and Te atoms with 1 to 1 ratio, arranging in a honeycomb manner and each occupying a sublattice. The STM image also rules out the possibility of Ag_2Te monolayer growth,[27] which would lead to a hexagonal lattice instead of honeycomb. A similar structure was recently proposed on another system, namely CuSe monolayer on Cu(111) substrate.[21] The schematic model in Fig. 2(c) shows ideally the superstructure of the (1×1) AgTe lattice on a $(\sqrt{3} \times \sqrt{3})$ Ag(111) substrate, with a rotation angle of 30°, leading to formation of the flat honeycomb structure.

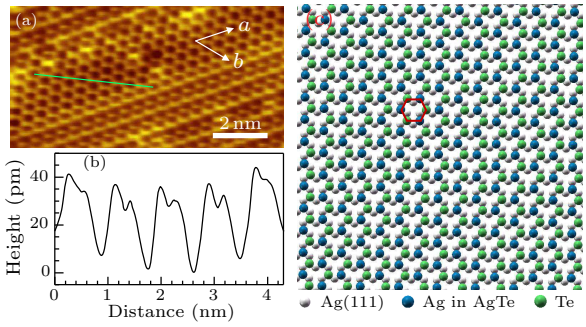

Fig. 2. (a) STM image of monolayer AgTe showing the flat honeycomb regions. Scanning parameters: $V_s = -0.6\,\mathrm{V}$, $I_t = 0.1\,\mathrm{nA}$. (b) Line profile of the honeycomb structure showing the asymmetric sublattices. (c) Schematic of the flat honeycomb structure of AgTe on Ag(111) substrate.

A large-scale STM image for a typical area with the alternating rows of ridges and trenches is shown in Fig. 3(a). Figure 3(b) is a zoom-in image of the "ridge" area. The tilted honeycomb structures appear in double rows, forming the buckled honeycomb area. A height profile is also shown in Fig. 3(c). The origin of the buckled honeycomb structure is not clear yet, and it didn't appear in the Cu–Se system.[20,21] Since we have mentioned the existence of intrinsic in-plane strain in the flat honeycomb, the buckled structure is likely the result of strain relief process. Another experimental evidence supporting this speculation is that we never find large area (e.g., with width >5 nm) of the flat honeycomb structure and that it always coexists with the buckled honeycomb area (Fig. 3(a)). Therefore, the flat honeycomb should be energetically less stable than the buckled honeycomb and the alternating rows of flat and buckled region relieves the strain at the AgTe-substrate interface.

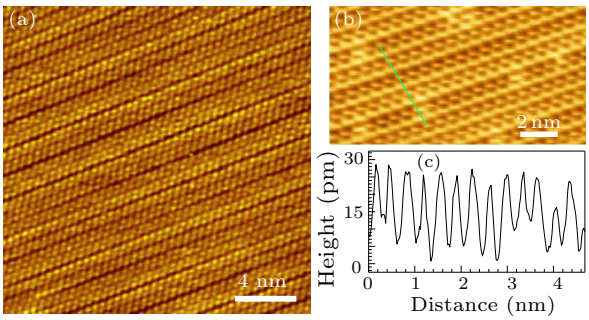

Fig. 3. (a) STM image of the buckled honeycomb regions. Scanning parameters: $V_s = -1.5\,\mathrm{V}$, $I_t = 0.4\,\mathrm{nA}$. (b) Zoom-in image of (a) showing the buckled honeycomb structure. Scanning parameters: $V_s = -0.6\,\mathrm{V}$, $I_t = 0.1\,\mathrm{nA}$. (c) Line profile of the buckled honeycomb structure.

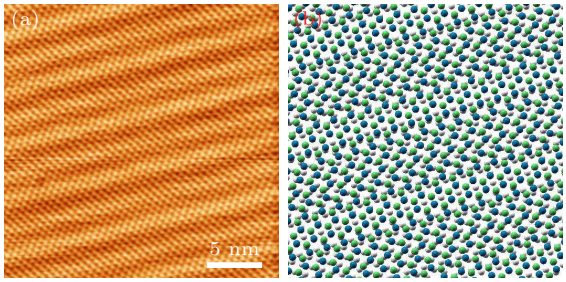

Fig. 4. (a) STM image showing the stripe structure. Scanning parameters: $V_s = -1.8\,\mathrm{V}$, $I_t = 0.8\,\mathrm{nA}$. (b) Schematic of the stripe formation of the AgTe on Ag(111) substrate.

Another way of relieving strain is the formation of stripe structures, as shown in Fig. 4(a). The stripe structure results from the distortion of the honeycomb lattice of the AgTe on Ag(111). Instead of forming the buckled double rows, the honeycomb lattice elongates along the stripe direction, leading to the formation of periodical 1D stripes (1D moiré pattern), as shown in Fig. 4(b). The stripe features give rise to the inner sets of the LEED spots in Fig. 1(b) and the outer sets of spots are caused by the honeycomb structure. We also note that the inner six spots shown in Fig. 1(b) are actually the third-order diffraction spots of the stripe

structure, and the first-order spots can only be clearly identified at lower beam energy of such as 25.7 eV. The area of the stripe structure can be much larger (>200 nm×200 nm) than the flat honeycomb region, due to a more stable geometry on the surface.

Given higher dosage of Te on Ag(111) substrate, the patterned hexagonal structure of the AgTe layer is observed. As shown in Figs. 5(a) and 5(b), the new structure is featured by the emergence of pseudo periodic array of holes, which is similar to another system studied previously.[20] The CuSe grown on Cu(111) substrate also shows that the removal of Cu and Se atoms gives rise to maximum gain of energy and leads to the formation of the ordered array of holes. In our system the holes are also formed since the removal of certain amount of the Ag and Te atoms stabilizes the whole structure. The honeycomb lattice can also be clearly identified in the atomic resolution image in Fig. 5(b). We would also like to note that our ongoing work about Cu_2Se system suggests no hole formation. The emergence of holes and the honeycomb lattice also support the formation of AgTe. Meanwhile, the distortion of the lattice can also be seen, giving rise to the formation of some triangular shaped regions. The formation of holes and the distortion of the lattice is also closely related to the strain in the AgTe film.

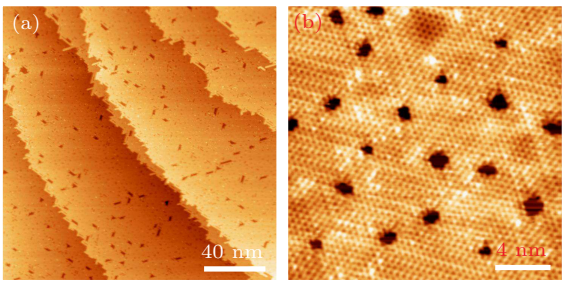

Fig. 5. (a) Large-scale and (b) atomic resolution STM images of the AgTe on Ag(111) with higher Te coverage, showing the patterned hexagonal structure of AgTe. Scanning parameters: $V_s = -1.8$ V, $I_t = 0.8$ nA.

In conclusion, we have succeeded in preparation of two-dimensional monolayer AgTe crystal on Ag(111) substrate. The STM and LEED results show that there are four kinds of atomic structures of the samples, which are due to the lattice mismatch, in-plane strain, the atomic interaction at the interface, and the two crystalline orientations. It would be interesting to further investigate the electronic structures of different surface areas of AgTe and also the boundaries between the regions. Further studies of the Ag–Te system on Ag(111) including manipulation of structure and physical property using different techniques are under the way. The fabrication of the novel two-dimensional monolayer AgTe crystal and its technique may pave the way to studying the novel physical properties and practical applications in future topological quantum devices.

References

[1] Novoselov K S, Geim A K, Morozov S V, Jiang D, Zhang Y, Dubonos S V, Grigorieva I V and Firsov A A 2004 *Science* **306** 666
[2] Novoselov K S, Mishchenko A, Carvalho A and Neto A H C 2016 *Science* **353** aac9439
[3] Pan Y, Zhang L Z, Huang L, Li L F, Meng L, Gao M, Huan Q, Lin X, Wang Y L, Du S X, Freund H J and Gao H J 2014 *Small* **10** 2215
[4] Zhang G Y, Du S X, Wu K H and Gao H J 2018 *Science* **360** 673
[5] Li G, Zhang Y Y, Guo H, Huang L, Lu H L, Lin X, Wang Y L, Du S X and Gao H J 2018 *Chem. Soc. Rev.* **47** 6073
[6] Zhang S L, Guo S Y, Chen Z F, Wang Y L, Gao H J, Gomez-Herrero J, Ares P, Zamora F, Zhu Z and Zeng H B 2018 *Chem. Soc. Rev.* **47** 982
[7] Pan Y, Shi D X and Gao H J 2007 *Chin. Phys.* **16** 3151
[8] Pan Y, Zhang H G, Shi D X, Sun J T, Du S X, Liu F and Gao H J 2009 *Adv. Mater.* **21** 2777
[9] Huang L, Xu W Y, Que Y D, Mao J H, Meng L, Pan L D, Li G, Wang Y L, Du S X, Liu Y Q and Gao H J 2013 *Chin. Phys. B* **22** 096803
[10] Meng L, Wang Y L, Zhang L Z, Du S X, Wu R T, Li L F, Zhang Y, Li G, Zhou H T, Hofer W A and Gao H J 2013 *Nano Lett.* **13** 685
[11] Huang L, Zhang Y F, Zhang Y Y, Xu W Y, Que Y D, Li E, Pan J B, Wang Y L, Liu Y Q, Du S X, Pantelides S T and Gao H J 2017 *Nano Lett.* **17** 1161
[12] Li G, Zhang L Z, Xu W Y, Pan J B, Song S R, Zhang Y, Zhou H T, Wang Y L, Bao L H, Zhang Y Y, Du S X, Ouyang M, Pantelides S T and Gao H J 2018 *Adv. Mater.* **30** 1804650
[13] Li L F, Lu S Z, Pan J B, Qin Z H, Wang Y Q, Wang Y L, Cao G Y, Du S X and Gao H J 2014 *Adv. Mater.* **26** 4820
[14] Wu X, Shao Y, Liu H, Feng Z, Wang Y L, Sun J T, Liu C, Wang J O, Liu Z L, Zhu S Y, Wang Y Q, Du S X, Shi Y G, Ibrahim K and Gao H J 2017 *Adv. Mater.* **29** 1605407
[15] Shao Y, Liu Z L, Cheng C, Wu X, Liu H, Liu C, Wang J O, Zhu S Y, Wang Y Q, Shi D X, Ibrahim K, Sun J T, Wang Y L and Gao H J 2018 *Nano Lett.* **18** 2133
[16] Zhu F F, Chen W J, Xu Y, Gao C L, Guan D D, Liu C H, Qian D, Zhang S C and Jia J F 2015 *Nat. Mater.* **14** 1020
[17] Zhang Z H, Penev E S and Yakobson B I 2017 *Chem. Soc. Rev.* **46** 6746
[18] Wang Q H, Kalantar-Zadeh K, Kis A, Coleman J N and Strano M S 2012 *Nat. Nanotechnol.* **7** 699
[19] Fatemi V, Wu S F, Cao Y, Bretheau L, Gibson Q D, Watanabe K, Taniguchi T, Cava R J and Jarillo-Herrero P 2018 *Science* **362** 926
[20] Lin X, Lu J C, Shao Y, Zhang Y Y, Wu X, Pan J B, Gao L, Zhu S Y, Qian K, Zhang Y F, Bao D L, Li L F, Wang Y Q, Liu Z L, Sun J T, Lei T, Liu C, Wang J O, Ibrahim K, Leonard D N, Zhou W, Guo H M, Wang Y L, Du S X, Pantelides S T and Gao H J 2017 *Nat. Mater.* **16** 717
[21] Gao L, Sun J T, Lu J C, Li H, Qian K, Zhang S, Zhang Y Y, Qian T, Ding H, Lin X, Du S and Gao H J 2018 *Adv. Mater.* **30** 1707055
[22] Anasori B, Lukatskaya M R and Gogotsi Y 2017 *Nat. Rev. Mater.* **2** 16098
[23] Wang Y, Xiao J, Zhu H Y, Li Y, Alsaid Y, Fong K Y, Zhou Y, Wang S Q, Shi W, Wang Y, Zettl A, Reed E J and Zhang X 2017 *Nature* **550** 487
[24] Zhang Y C and Stucky G D 2014 *Chem. Mater.* **26** 837
[25] van Veggel F C J M 2014 *Chem. Mater.* **26** 111
[26] Zhang W, Yu R, Feng W X, Yao Y G, Weng H M, Dai X and Fang Z 2011 *Phys. Rev. Lett.* **106** 156808
[27] Ma Y D, Kou L Z, Dai Y and Heine T 2016 *Phys. Rev. B* **93** 235451
[28] Zhang Y H, Li Y, Ma Y M, Li Y W, Li G H, Shao X C, Wang H, Cui T, Wang X and Zhu P W 2015 *Sci. Rep.* **5** 14681
[29] Sáfrán G, Geszti O, Radnóczi G 2003 *Vacuum* **71** 299